Identification of a PET Radiotracer for Imaging of the Folate Receptor-α: A Potential Tool to Select Patients for Targeted Tumor Therapy

Patrycja Guzik[1], Hsin-Yu Fang[1], Luisa M. Deberle[1], Martina Benešová[1,2], Susan Cohrs[1], Silvan D. Boss[2], Simon M. Ametamey[2], Roger Schibli[1,2], and Cristina Müller[1,2]

[1]*Center for Radiopharmaceutical Sciences, Paul Scherrer Institute, Villigen-PSI, Switzerland; and* [2]*Department of Chemistry and Applied Biosciences, ETH Zurich, Zurich, Switzerland*

The aim of this study was to identify a folate receptor-α (FRα)–selective PET agent potentially suitable for the selection of patients who might profit from FRα-targeted therapies. The 6*R* and 6*S* isomers of ^{18}F-aza-5-methyltetrahydrofolate (MTHF) were assessed regarding their binding to FRα and FRβ, expressed on cancer and inflammatory cells, respectively, and compared with ^{18}F-AzaFol, the folic acid–based analog. **Methods:** FR selectivity was investigated using FRα-transfected (RT16) and FRβ-transfected (D4) CHO cells. The cell uptake of ^{18}F-folate tracers was investigated, and receptor-binding affinities were determined with the nonradioactive analogs. In vitro autoradiography of the ^{18}F-folate tracers was performed using RT16 and D4 tissue sections. Biodistribution studies and PET/CT imaging of the radiotracers were performed on mice bearing RT16 and D4 xenografts. **Results:** The uptake of ^{18}F-6*R*-aza-5-MTHF was high when using RT16 cells (62% ± 10% of added activity) but much lower when using D4 cells (5% ± 2%). The FRα selectivity of ^{18}F-6*R*-aza-5-MTHF was further demonstrated by its approximately 43-fold higher binding affinity to FRα (half-maximal inhibitory concentration [IC_{50}], 1.8 ± 0.1 nM) than to FRβ (IC_{50}, 77 ± 27 nM). The uptake of ^{18}F-6*S*-aza-5-MTHF and ^{18}F-AzaFol was equal in both cell lines (52%–70%), with similar affinities to FRα (IC_{50}, 2.1 ± 0.4 nM and 0.6 ± 0.3 nM, respectively) and FRβ (0.8 ± 0.2 nM and 0.3 ± 0.1 nM, respectively). The autoradiography signal obtained with ^{18}F-6*R*-aza-5-MTHF was 11-fold more intense for RT16 than for D4 tissue sections. Biodistribution data showed high uptake of ^{18}F-6*R*-aza-5-MTHF in RT16 xenografts (81% ± 20% injected activity per gram [IA]/g 1 h after injection) but significantly lower accumulation in D4 xenografts (7.3% ± 2.1% IA/g 1 h after injection), which was also visualized using PET. The uptake of ^{18}F-6*S*-aza-5-MTHF and ^{18}F-AzaFol was similar in RT16 (53% ± 10% IA/g and 45% ± 2% IA/g, respectively) and D4 xenografts (77% ± 10% IA/g and 52% ± 7% IA/g, respectively). **Conclusion:** This study demonstrated FRα selectivity for ^{18}F-6*R*-aza-5-MTHF but not for ^{18}F-6*S*-aza-5-MTHF or ^{18}F-AzaFol. This characteristic, together with its favorable tissue distribution, makes ^{18}F-6*R*-aza-5-MTHF attractive for clinical translation to enable detection of FRα-positive cancer while preventing undesired accumulation in FRβ-expressing inflammatory cells.

Key Words: folate receptor (FR); 5-MTHF; PET; ^{18}F; FRα selectivity

J Nucl Med 2021; 62:1475–1481
DOI: 10.2967/jnumed.120.255760

Received Oct. 17, 2020; revision accepted Jan. 13, 2021.
For correspondence or reprints, contact Cristina Müller (cristina.mueller@psi.ch).
Published online January 15, 2021.

The folate receptor-α (FRα) is a cell membrane–associated protein that has been used for targeted therapies in oncology (*1*). The FRα-expressing malignancies are mainly gynecologic cancers, such as ovarian, endometrial, and cervical tumors, but non–small cell lung cancer, triple-negative breast cancer, and kidney cancer were also reported to be frequently positive for FRα (*2–6*).

The use of folic acid–based radiotracers for nuclear imaging was proposed for diagnosis of FR-positive cancer and for the selection of patients who would profit from FR-targeted tumor therapies (*7–10*). ^{111}In-DTPA-folate and ^{99m}Tc-EC20 suitable for SPECT were the first two folate radioconjugates tested in patients (*8,11,12*). Folic acid–based radiotracers bind to both FRα and FRβ, which have distinct tissue expression profiles (*13,14*). The FRα is present in malignant tissue (*15*), whereas FRβ is expressed mainly on activated macrophages involved in inflammatory diseases (*16*). As a result, folic acid–based radiotracers accumulate not only in tumors but also at sites of inflammation, which may result in false-positive findings due to coexisting inflammatory conditions in cancer patients.

6*S*/6*R*-5-methyltetrahydrofolates (MTHF) are reduced folate forms, in contrast to folic acid, which is the synthetic, oxidized version of folate vitamins. It was previously reported that the physiologic 6*S*-5-MTHF, but not the 6*R*-5-MTHF, binds with approximately 50-fold higher affinity to FRα than to FRβ (*17,18*). In a proof-of-concept study published by Vaitilingam et al., a dimethylated reduced version of ^{99m}Tc-EC20 was prepared to achieve FRα selectivity (*19*). Indeed, it was experimentally demonstrated that ^{99m}Tc-DMTHF, a reduced form of ^{99m}Tc-EC20, accumulated much more in tumors of mice than at sites of inflammation (*19*).

In view of a clinical application, folate radiotracers for PET imaging would be clearly favored (*20,21*). ^{18}F-based radiotracers profit from the favorable decay characteristics of ^{18}F (half-life, 110 min; average $E\beta^+$, 250 keV) and the option of quantifying the accumulated activity using standard protocols that are also used for interventions with ^{18}F-FDG (*22*).

Among a large number of developed ^{18}F-folate tracers (*21*) only two were used in clinics. Verweij et al. reported on the use of ^{18}F-polyethylene glycol folate for macrophage imaging in patients with rheumatoid arthritis (*23*), whereas ^{18}F-AzaFol has recently been tested in a clinical phase I trial in ovarian and lung cancer patients in Switzerland (NCT0342993) (*24,25*). A tumor-selective ^{18}F-folate tracer for PET that targets solely FRα and not FRβ would be essential to unambiguously identify patients who could profit from FRα-targeted therapies.

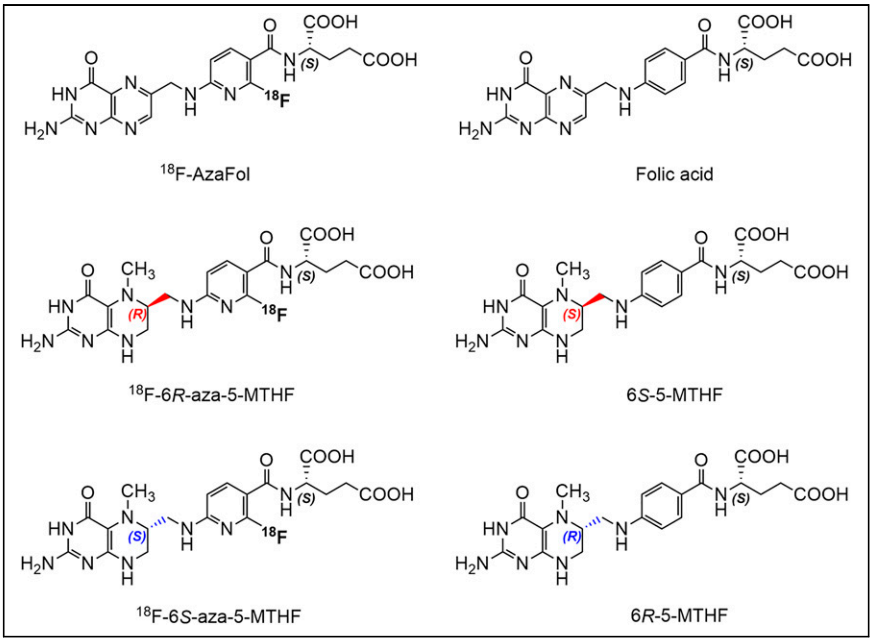

FIGURE 1. Chemical structures of ^{18}F-AzaFol, ^{18}F-6*R*-aza-5-MTHF, and ^{18}F-6*S*-aza-5-MTHF, as well as folic acid, 6*S*-5-MTHF, and 6*R*-5-MTHF (*26*). Stereochemical nomenclature of corresponding isomers of nonfluorinated and fluorinated 5-MTHFs are inversed because of change in substituents' priority at stereogenic center.

We have previously developed radiotracers based on 6*S*- and 6*R*-5-MTHF as a targeting agent (*26*), in which the ^{18}F-label was integrated in the folate backbone as was the case for ^{18}F-AzaFol (Fig. 1) (*26*). These 5-MTHF–based ^{18}F-tracers accumulated to a higher extent in tumor xenografts of mice than did ^{18}F-AzaFol, and the 6*R* isomer even showed a favorable excretion profile. The goal of the present study was, therefore, to investigate ^{18}F-6*R*-aza-5-MTHF and ^{18}F-6*S*-aza-5-MTHF with regard to their binding affinity to FRα and FRβ, in order to assess the potential of using them for tumor-selective PET imaging.

MATERIALS AND METHODS

Folate Derivatives

The precursors (6*R*- or 6*S*-N^2-acetyl-3'-aza-2'-chloro-5-MTHF di-*tert*-butylester and N^2-acetyl-3'-aza-2'-chlorofolic acid di-*tert*-butylester) for the radiofluorination and the nonradioactive 6*S*-5-MTHF (physiologic form) and 6*R*-5-MTHF (nonphysiologic form) were provided by Merck & Cie. Folic acid was obtained from Sigma-Aldrich. The nonradioactive fluoro-folates, as well as 6*R*-3'-aza-2'-^{18}F-5-MTHF (^{18}F-6*R*-aza-5-MTHF), 6*S*-3'-aza-2'-^{18}F-5-MTHF (^{18}F-6*S*-aza-5-MTHF), and 3'-aza-2'-^{18}F-folic acid (^{18}F-AzaFol), were synthesized at ETH Zurich according to a previously reported method (*24,26*). The molar activity of the radiotracers was in the range of 20–250 GBq/μmol, with commonly higher values for ^{18}F-AzaFol than for the 5-MTHF–based radiotracers (*24,26*). ^{3}H-folic acid was obtained from Moravek Biochemicals, Inc.

Cell Culture

CHO cells transfected with FRα (designated as RT16) or FRβ (designated as D4) were kindly provided by Prof. Larry H. Matherly of Wayne State University (*27*). The cells were cultured in folate-free minimal essential medium-α. KB cells (FR-positive human cervical carcinoma cell line, ACC-136) were obtained from the German Collection of Microorganisms and Cell Cultures (DSMZ GmbH) and cultured in folate-deficient RPMI medium. PC-3 cells (FR-negative human prostate cancer cell line, ACC-465) were also obtained from DSMZ but cultured in normal RPMI 1640 medium. The cell culture media were supplemented with 10% fetal calf serum, L-glutamine, and antibiotics.

Western Blot

Expression of FRα and FRβ in RT16 and D4 cells, respectively, was verified by Western blot analysis, whereas FRα -expressing KB and FR-negative PC-3 tumor cells were used as positive and negative controls, respectively. Cell protein extracts (30 μg/well) were separated by sodium dodecyl sulfate–polyacrylamide gel electrophoresis and transferred to a polyvinylidene difluoride membrane. After blocking with 5% bovine serum albumin (BSA) solution, the membrane was incubated with a primary anti-FRα antibody (1:625 rabbit monoclonal antibody PA5-42004; Invitrogen) or anti-FRβ antibody (1:1,000 rabbit monoclonal antibody GTX105822; GeneTex) overnight at 4°C. For signal detection, a secondary antirabbit IgG antibody functionalized with horseradish peroxidase was used together with chemiluminescent substrate. Detection of β-actin served as a loading control (anti-β-actin antibody: 1:2,000 mouse monoclonal antibody 3700 [Cell Signaling Technology] and 1:5,000 horseradish peroxidase–conjugated antimouse IgG 7076S [Cell Signaling Technology]). The expression of FRα and FRβ on RT16 and D4 cells, respectively, was assessed by comparison of the signal with that of KB cells and shown on one representative Western blot.

Cell Internalization of ^{18}F-6*R*/6*S*-Aza-5-MTHF and ^{18}F-Azafol

Cell uptake of ^{18}F-6*R*-aza-5-MTHF, ^{18}F-6*S*-aza-5-MTHF, and ^{18}F-AzaFol was determined as previously reported (*26,28*). In brief, RT16 and D4 cells were seeded in poly-L-lysine–coated 12-well plates to form confluent monolayers overnight. The cells were incubated with the ^{18}F-folate radiotracer (~200 kBq; 25 μL) with or without excess folic acid (~100 μM) for 3 h at 37°C. The results were expressed as percentage of total added activity. The statistical significance was assessed using a two-way ANOVA with a Tukey multiple comparisons posttest using GraphPad Prism software (version 7.0). A P value of less than 0.05 was considered statistically significant.

FRα- and FRβ-Binding Affinity (Half-Maximal Inhibitory Concentration [IC_{50}] Values)

The IC_{50} values for FRα and FRβ were determined in displacement experiments using nonradioactive fluoro-folates (^{19}F-6*R*-aza-5-MTHF, ^{19}F-6*S*-aza-5-MTHF, and ^{19}F-AzaFol) and ^{3}H-folic acid as previously reported (*24*). The binding affinities of the corresponding nonfluorinated analogs (6*R*-5-MTHF, 6*S*-5-MTHF, and folic acid) were determined for comparison. The folate derivatives of interest were applied in a concentration range of 5 pM–50 μM (Supplemental Table 1; supplemental materials are available at http://jnm.snmjournals.org). The FR-bound fraction of ^{3}H-folic acid was measured using a β-counter (Packard Bioscience Cobra II). The IC_{50} values were determined by nonlinear regression analysis of displacement curves obtained from at least three independent experiments, using GraphPad Prism software. For comparison, the relative affinities of ^{19}F-6*S*-aza-5-MTHF and ^{19}F-

6*R*-aza-5-MTHF were presented as a percentage of the binding affinity determined for ^{19}F-AzaFol (set as 100%). The receptor-binding affinities of 6*R*-5-MTHF and 6*S*-5-MTHF were expressed relative to the determined binding affinity of folic acid (set as 100%).

Autoradiography Studies

Autoradiography studies were performed using tissue sections of RT16, D4, KB, and PC-3 xenografts as previously reported (*29*). The sections were incubated in Tris-HCl buffer containing 0.25% BSA. After removal of the buffer, the sections were incubated for 1 h at room temperature with the ^{18}F-folate radiotracers (150 kBq/100 μL) in Tris-buffer containing 1% BSA with or without addition of excess folic acid (100 μM). Autoradiographic images were obtained using a storage phosphor system (Cyclone Plus; Perkin Elmer) and quantified using OptiQuant software (version 5.0). The signals obtained from RT16, D4, and PC-3 xenograft sections were normalized to the signal obtained from a KB xenograft section (set as 100%). The resulting values of ^{18}F-6*R*-aza-5-MTHF and ^{18}F-6*S*-aza-5-MTHF were expressed relative to the signal of ^{18}F-AzaFol, which was set as 100%. Representative images were prepared using ImageJ (version 1.52d).

Immunohistochemistry

After deparaffinization, rehydration, and antigen retrieval of the xenograft sections (RT16, D4, and KB), the slides were treated with 3.5% hydrogen peroxide, followed by endogenous biotin blockade using avidin solution (avidin/biotin blocking kit SP-2001; Vector Laboratories) in an aqueous solution of 3% BSA and normal 5% goat serum. The sections were incubated with an anti-FRα antibody (PA5-42004; Invitrogen) and an anti-FRβ antibody (GTX105822; GeneTex) diluted 1:800 and 1:400, respectively, in biotin solution mixed with 3% BSA at 4°C overnight. Afterward, the sections were incubated with the secondary antibody (goat antirabbit IgG, BA-1000; Vector Laboratories) diluted 1:1,000 and 1:500 in phosphate-buffered saline containing 3% BSA. Signal was visualized using reagents of commercial kits (Vectostain Elite ABC-horseradish peroxidase kit, peroxidase PK-6100, and 3,3′-diaminobenzidine substrate kit peroxidase (horseradish peroxidase) SK-4100; Vector Laboratories), followed by counterstaining using hematoxylin. After tissue dehydration, the sections were fixed with xylene and images were taken using a light microscope (Axio Lab.A1; Zeiss).

In Vivo Studies

All applicable international, national, and institutional guidelines for the care and use of laboratory animals were followed. The studies were performed according to the guidelines of the Swiss Regulations for Animal Welfare after ethical approval by the Cantonal Committee of Animal Experimentation and permission by the responsible authorities. Female severe combined immunodeficient CB17 mice were purchased from Charles River Laboratories. All animals were fed with a folate-deficient rodent diet (ssniff Spezialdiäten GmbH). The mice were inoculated with RT16 cells (6×10^6 cells in 100 μL of phosphate-buffered saline) on the right shoulder and D4 cells (6×10^6 cells in 100 μL of phosphate-buffered saline) on the left shoulder. Biodistribution and PET/CT imaging studies were performed 8–10 d later.

Biodistribution Studies

The respective ^{18}F-folate radiotracer (~5 MBq, 100 μL, ~0.2 nmol) was injected into the lateral tail vein, and the mice were sacrificed at 1 or 3 h after injection. Selected tissues and organs were collected and weighed, and the activity was measured using a γ-counter (Wallac Wizard 1480; Perkin Elmer). The results for 3–4 mice per time point were listed as a percentage of the injected activity (IA) per gram of tissue mass, using counts of a standard solution (5% IA) measured at the same time. The datasets were analyzed for significance using a one-way ANOVA with a Tukey multiple comparison posttest using GraphPad Prism software. A P value of less than 0.05 was considered statistically significant.

PET/CT Imaging Studies

PET/CT scans were performed using a small-animal PET/CT scanner (G8; Perkin Elmer (*30*)) as previously reported (*26*). After emptying the urinary bladder of the mice, they were anesthetized with a mixture of isoflurane (1.5%–2.0%) and oxygen for PET/CT acquisitions. Static whole-body PET scans of 10-min duration were obtained at 1 and 3 h after intravenous injection of ^{18}F-folate radiotracers (5 MBq, ~0.2 nmol, 100 μL), followed by a CT scan of 1.5 min. The acquisition of the data and their reconstruction was performed using the G8 PET/CT scanner software (version 2.0.0.10). The images show one representative example for each radiotracer, prepared using VivoQuant postprocessing software (version 3.5; inviCRO Imaging Services and Software).

RESULTS

Uptake of ^{18}F Radiotracers in FRα-Positive RT16 and FRβ-Positive D4 Cells

Western blot analysis unambiguously confirmed FRα expression on RT16 cells and FRβ expression on D4 cells by detection of the bands at 38 and 29 kDa, respectively (Fig. 2A). The quantified signal for FRα on RT16 cells and FRβ on D4 cells was in the range of 20%–45% of the FRα signal of KB cells. Only a weak signal of 6%–7% was obtained for FRα on D4 cells and FRβ on RT16 cells. This was in the same range as the signal for PC-3 cells (5%–6%), which are FR-negative (Supplemental Fig. 1) (*31*).

The uptake of ^{18}F-6*R*-aza-5-MTHF (62% ± 10% of total added activity) and ^{18}F-6*S*-aza-5-MTHF (64% ± 15%) into RT16 cells was in the same range as for ^{18}F-AzaFol (52% ± 4%) after a 3-h incubation period ($P > 0.05$). The internalized fractions of all three radiotracers were in the range of 11%–13% of total added activity ($P > 0.05$). FRα-specific uptake was confirmed by complete blockade of radiotracer uptake in cell samples preincubated with excess folic acid (Fig. 2B). Experiments performed on D4 cells showed significantly lower uptake of ^{18}F-6*R*-aza-5-MTHF (5% ± 2%; $P < 0.05$) than of ^{18}F-6*S*-aza-5-MTHF (70% ± 7%) or ^{18}F-AzaFol (61% ± 14%), which were both in the same range ($P > 0.05$). Coincubation of D4 cells with excess folic acid reduced the uptake of all radiotracers to background levels (<0.1%) (Fig. 2B).

FRα and FRβ Binding Affinities

The binding affinity of ^{19}F-6*R*-aza-5-MTHF to FRα was approximately 40-fold higher (IC_{50} value, 1.8 ± 0.1 nM) than that to FRβ (77 ± 27 nM). In contrast, the binding affinity of ^{19}F-6*S*-aza-5-MTHF to both FR isoforms was similar (2.1 ± 0.4 nM and 0.8 ± 0.2 nM, respectively), and the same held true also for ^{19}F-AzaFol (0.6 ± 0.3 nM and 0.3 ± 0.1 nM, respectively). These findings corresponded well with the determined values of the respective nonfluorinated analogs, demonstrating an approximately 70-fold higher binding of 6*S*-5-MTHF to FRα than to FRβ but equal binding affinities to both FR isoforms for 6*R*-5-MTHF and folic acid (Table 1; Supplemental Fig. 2).

Determination of the FRα-binding affinity of ^{19}F-6*R*-aza-5-MTHF and ^{19}F-6*S*-aza-5-MTHF relative to ^{19}F-AzaFol (set as 100%) revealed a lower value for the reduced folates (29%–34%), which was in line with the results obtained for nonfluorinated 6*S*-5-MTHF and 6*R*-5-MTHF relative to folic acid (28%–44%). The relative binding affinity to FRβ was 300-fold lower for ^{19}F-6*R*-aza-5-MTHF than for ^{19}F-AzaFol, whereas the FRβ-binding affinity of ^{19}F-6*S*-aza-5-MTHF was only slightly reduced, which

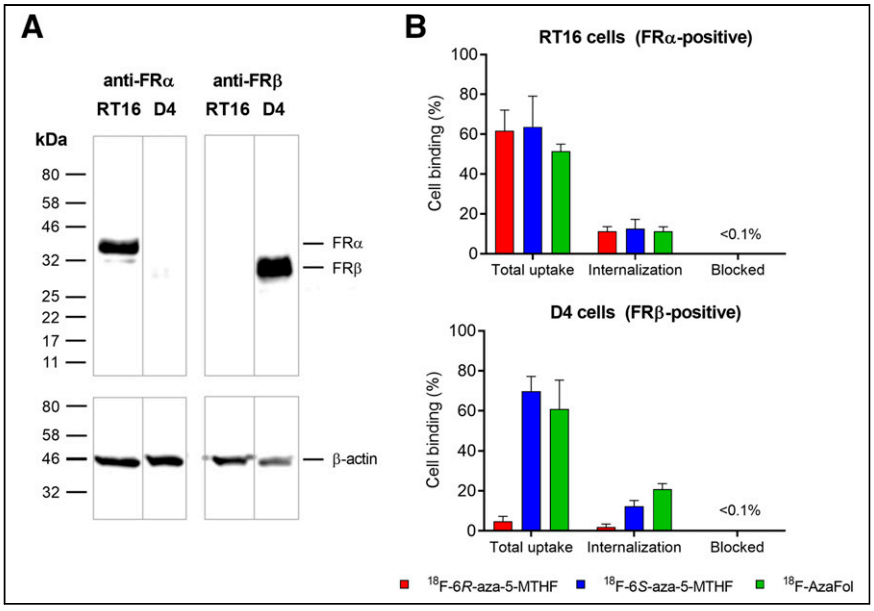

FIGURE 2. (A) Western blot analysis of FRα expression in RT16 cell lysates and FRβ expression in D4 cell lysates (top panel). β-Actin staining as loading control (bottom panel). (B) Cell uptake and internalization of ^{18}F-6*R*-aza-5-MTHF, ^{18}F-6*S*-aza-5-MTHF, and ^{18}F-AzaFol in RT16 and D4 cells after 3 h of incubation at 37°C. Unspecific binding of radiotracers (blocked) was determined by coincubation of cells with folic acid (100 μM). Results are presented as average ± SD (n = 3).

corresponded well with the binding affinities of the nonfluorinated folates to FRβ relative to folic acid (Table 1).

Autoradiography Studies Using ^{18}F-Folate Tracers

In vitro autoradiography studies revealed a similar signal intensity on RT16 xenograft sections for ^{18}F-6*R*-aza-5-MTHF (74% ± 28%) and ^{18}F-6*S*-aza-5-MTHF (89% ± 33%), which was comparable to the signal of ^{18}F-AzaFol (set as 100%) (Fig. 3). A similar binding pattern was obtained with FRα-positive KB xenograft sections (Supplemental Fig. 3). The images obtained with D4 xenograft sections demonstrated, however, an over 10-fold lower signal for ^{18}F-6*R*-aza-5-MTHF (7% ± 4%; $P < 0.05$) than for ^{18}F-6*S*-aza-5-MTHF (81% ± 36%) relative to ^{18}F-AzaFol (set as 100%). Coincubation of ^{18}F-folates with excess folic acid to block the FR-specific binding resulted in only background signals, comparable to those obtained for FR-negative PC-3 tissue (Supplemental Fig. 3).

The expression of FRα on RT16 (and KB as a positive control) and FRβ on D4 xenograft sections was verified by a positive immunohistochemical staining result using an anti-FRα antibody and anti-FRβ antibody. The nonspecific binding was determined in the absence of the primary antibody (Supplemental Fig. 4).

Biodistribution of ^{18}F-Folate Tracers

Biodistribution studies were performed on RT16/D4 xenograft-bearing mice. At 1 and 3 h after injection of ^{18}F-6*R*-aza-5-MTHF, the uptake into FRα-positive RT16 xenografts ranged from 81% to 94% IA/g and was significantly higher than the uptake into FRβ-positive D4 xenografts (7.3%–7.6% IA/g; $P < 0.05$) (Fig. 4). The accumulation of ^{18}F-6*S*-aza-5-MTHF was in the same range for both xenograft types (RT16: 53%–122% IA/g; D4: 77%–149% IA/g), which was also the case for ^{18}F-AzaFol (RT16: 26%–45% IA/g; D4: 28%–52% IA/g) (Fig. 4). The increased uptake of 5-MTHF–based ^{18}F-folate tracers in FRα-positive RT16 xenografts, compared with the uptake of ^{18}F-AzaFol, was in line with previous data obtained from KB tumor–bearing nude mice (*26*).

The presented data, obtained for severe combined immunodeficient CB17 mice, showed a 3-fold lower renal retention of ^{18}F-6*R*-aza-5-MTHF (11%–25% IA/g) than of ^{18}F-6*S*-aza-5-MTHF (31%–41% IA/g) or ^{18}F-AzaFol (35%–58% IA/g), as previously observed in nude mice (Supplemental Tables 2–4) (*26*).

PET/CT Imaging Studies Using ^{18}F-Folate Tracers

Mice bearing RT16 and D4 xenografts on the right and left shoulders, respectively, were imaged at 1 and 3 h after injection of

TABLE 1
FR-Binding Affinities of Fluorinated and Nonfluorinated (Aza)-5-MTHF Derivatives Relative to ^{19}F-Azafol or Folic Acid, Respectively (Set as 100%), Determined with FRα-Expressing RT16 Cells and FRβ-Expressing D4 Cells

Compound	Relative affinity to FRα	Relative affinity to FRβ
^{19}F-AzaFol	100% (0.6 ± 0.3 nM)	100% (0.3 ± 0.1 nM)
^{19}F-6*R*-aza-5-MTHF	34% (1.8 ± 0.1 nM)	0.3% (77 ± 27 nM)
^{19}F-6*S*-aza-5-MTHF	29% (2.1 ± 0.4 nM)	32% (0.8 ± 0.2 nM)
Folic acid	100% (0.4 ± 0.2 nM)	100% (0.3 ± 0.1 nM)
6*S*-5-MTHF*	44% (0.9 ± 0.3 nM)	0.4% (64 ± 10 nM)
6*R*-5-MTHF*	28% (1.4 ± 0.5 nM)	34% (0.8 ± 0.4 nM)

*Stereochemical nomenclature of corresponding isomers of nonfluorinated 5-MTHFs are inversed because of different priority of substituents at the stereogenic center.

Data in parentheses represent the absolute binding affinities.

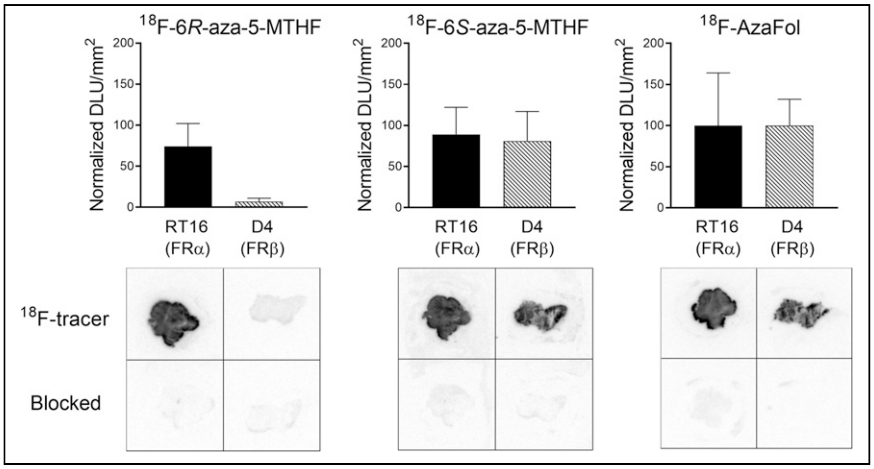

FIGURE 3. Signal intensities (normalized digital light units [DLU] per area [mm^2]) of ^{18}F-6*R*-aza-5-MTHF, ^{18}F-6*S*-aza-5-MTHF, and ^{18}F-AzaFol (set as 100%) quantified on the basis of RT16 (left) or D4 (right) autoradiography images. Bottom panel demonstrates FR blockade performed with excess folic acid.

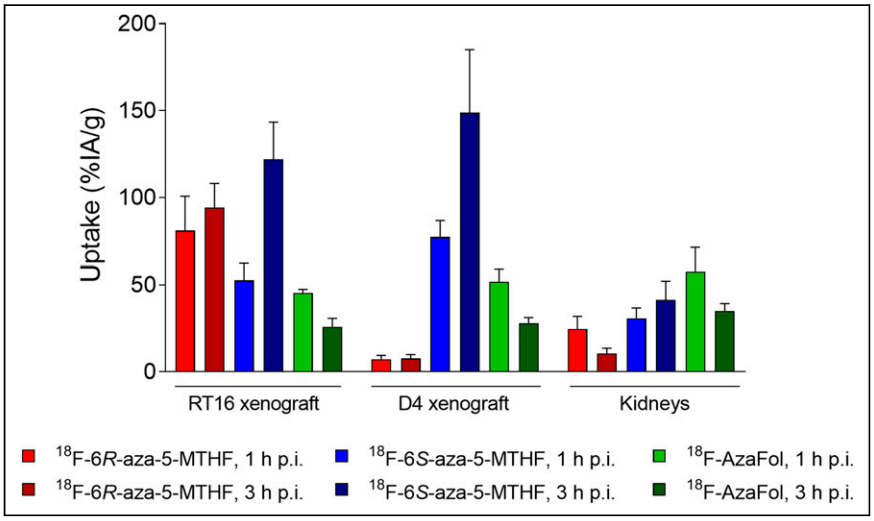

FIGURE 4. Graph representing uptake of ^{18}F-6*R*-aza-5-MTHF (red), ^{18}F-6*S*-aza-5-MTHF (blue), and ^{18}F-AzaFol (green) in RT16 and D4 xenografts and in kidneys at 1 and 3 h after injection of ^{18}F-folate radiotracers (5 MBq/mouse). p.i. = after injection.

the ^{18}F-folate radiotracers using preclinical PET/CT (Fig. 5). In agreement with the biodistribution data, a selective accumulation of ^{18}F-6*R*-aza-5-MTHF in the RT16 xenograft was readily visualized on PET/CT images. This finding was in clear contrast to the images obtained after injection of ^{18}F-6*S*-aza-5-MTHF and ^{18}F-AzaFol, which accumulated equally in RT16 and D4 xenografts. The PET images further confirmed the previously published data that showed much lower kidney retention of ^{18}F-6*R*-aza-5-MTHF than of ^{18}F-6*S*-aza-5-MTHF or ^{18}F-AzaFol (*26*). The RT16 xenograft-to-kidney ratios were, thus, considerably higher for the 6*R* isomer than for the 6*S* isomer, whereas the opposite held true for the xenograft-to-liver ratios.

DISCUSSION

FR-targeted cancer therapies, including folic acid–drug conjugates (e.g., vintafolide (*32,33*)), FRα -targeted antibodies (e.g., farletuzumab (*34*)), or FRα antibody–drug conjugates (e.g., mirvetuximab soravtansine (*35*)), hold promise for the treatment of patients with FRα -positive tumors (*1,8*). The response to these therapies will, however, critically depend on the patient inclusion criteria, which should consider only those cases in which most lesions are FRα -positive (*36*). Although ^{18}F-AzaFol visualizes FR-positive tissue on PET images (*25*), false-positive results may occur because of concomitant accumulation of the radiotracer in FRβ-expressing macrophages involved at sites of inflammation. Having a means at hand to provide a full picture of FRα-positive lesions in an individual patient would thus present an essential step toward the success of any FRα-targeted cancer therapy concept (*1,8*).

In this study, we have demonstrated that ^{19}F-6*R*-aza-5-MTHF displayed significantly higher affinity to FRα than to FRβ, indicating the anticipated FRα selectivity. These findings agree with those obtained from the corresponding nonfluorinated versions of 5-MTHF, confirming the original observation of Wang et al., who reported 6*S*-5-MTHF to have an approximately 50-fold higher affinity to FRα than to FRβ (*17,18*). However, folic acid and the nonphysiologic 6*R*-5-MTHF, as well as their fluorinated analogs, showed equal binding to both FR isoforms.

The fact that only the 6*R* isomer—not the 6*S* isomer—of the novel aza-5-MTHF–based ^{18}F-folate tracers bound with higher affinity to FRα than to FRβ is an essential finding. It indicates the need for diastereomerically pure folate radiotracers other than previously proposed by the development of a racemic mixture of ^{99m}Tc-DMTHF (*19*).

The in vivo evaluation of tumor-specific folate radiotracers in the presence of inflammation is challenging in mice, since the number of activated macrophages is commonly low and, hence, the expected signal from inflammatory sites is lower than the signal from the tumor tissue. This situation may complicate the interpretation of the results with regard to FRα selectivity. To unambiguously determine whether the ^{18}F-folate radiotracers accumulated specifically in FRα -expressing tissue, we have established a mouse model using RT16 and D4 cells to grow xenografts of comparable volumes. Using these mice enabled the determination of FRα-selective uptake of ^{18}F-6*R*-aza-5-MTHF in RT16 xenografts, whereas the accumulation in D4 xenografts was significantly lower. In contrast, ^{18}F-6*S*-aza-5-MTHF and ^{18}F-AzaFol showed comparable accumulation in both xenografts.

It is important to recognize that in addition to the FRα-selective accumulation of ^{18}F-6*R*-aza-5-MTHF, this radiotracer also showed the most favorable clearance from background tissues, including the kidneys as previously demonstrated by Boss et al., who

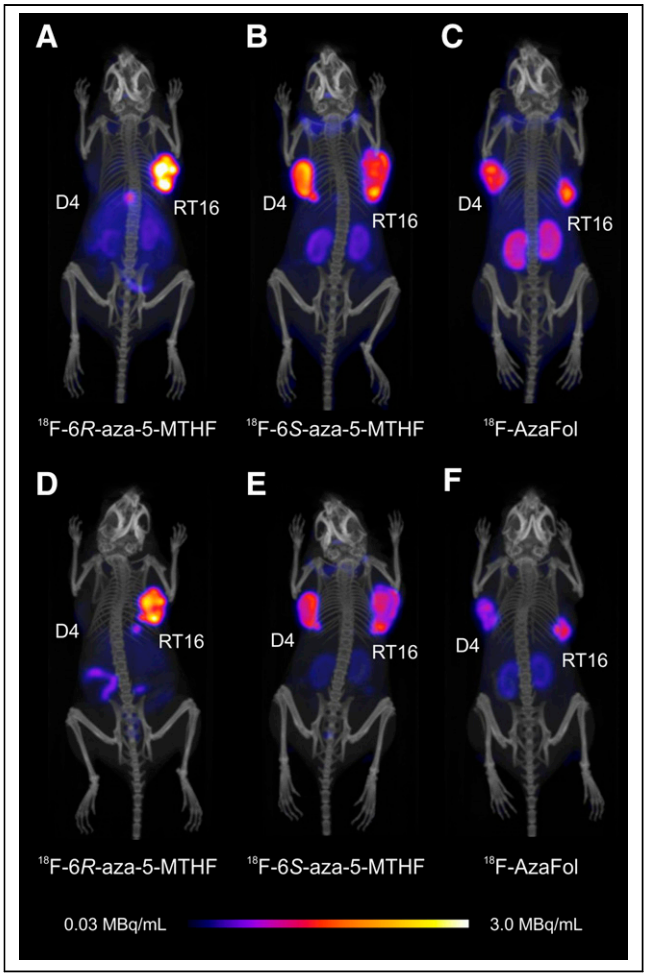

FIGURE 5. PET/CT images of mice bearing RT16 and D4 xenografts 1 h (A–C) and 3 h (D–F) after injection of ^{18}F-folate radiotracers (5 MBq/mouse) shown as maximum-intensity projections.

used KB tumor–bearing nude mice (*26*). The somewhat decreased FRα-binding affinity of the 5-MTHF–based ^{18}F radiotracers, as compared with the affinity of ^{18}F-AzaFol, is in line with the common knowledge that reduced folates display lower FR-binding affinity than does folic acid (*15,17,18*). Although the high FR-binding affinity of folic acid was postulated as a particular advantage of FR-targeting agents, we believe that 5-MTHF–based ^{18}F radiotracers may be favorably used for this purpose as they may be more efficiently released from FR after internalization (*37*). This could explain the higher uptake of ^{18}F-6*R*-aza-5-MTHF and ^{18}F-6*S*-aza-5-MTHF than of ^{18}F-AzaFol in RT16 and KB xenografts (*26*).

CONCLUSION

In this study, we have identified ^{18}F-6*R*-aza-5-MTHF as a novel PET agent that accumulated in FRα-positive RT16 xenografts but not in FRβ-positive D4 xenografts grown in the same mouse. The favorable tissue distribution profile of ^{18}F-6*R*-aza-5-MTHF, together with the herein-determined FRα selectivity, means a breakthrough in the field. PET imaging using ^{18}F-6*R*-aza-5-MTHF might serve as a way to unambiguously identify patients who can profit from FRα-targeted therapies; thus, ^{18}F-6*R*-aza-5-MTHF's potential for clinical translation deserves the highest attention.

DISCLOSURE

A patent application for ^{18}F-based folate radiotracers has been filed by Merck & Cie, Inc., whereby Roger Schibli, Simon M. Ametamey, Silvan D. Boss, and Cristina Müller are coinventors. The project was financially supported by Merck & Cie, Inc. (Schaffhausen, Switzerland), and by the Swiss National Science Foundation (grants 310030_156803 and 310030_188968). Patrycja Guzik was financially supported by a Swiss Government Excellence Scholarship. No other potential conflict of interest relevant to this article was reported.

ACKNOWLEDGMENTS

We thank Anna Becker, Raffaella Schmid, and Fan Sozzi-Guo for technical assistance with the experiments, and we thank Annette Krämer for producing the ^{18}F-based radiotracers at ETH Zurich.

KEY POINTS

QUESTION: Are 5-MTHF–based PET agents specific for the tumor-associated FRα?

PERTINENT FINDINGS: The data from this preclinical study confirm that ^{18}F-6*R*-aza-5-MTHF binds specifically to FRα, which makes this radiotracer useful as a tumor-specific PET agent.

IMPLICATIONS FOR PATIENT CARE: A PET imaging agent such as ^{18}F-6*R*-aza-5MTHF for the unambiguous identification of FRα-expressing tumor types will be essential for the selection of patients who might profit from FRα-targeted therapies.

REFERENCES

1. Scaranti M, Cojocaru E, Banerjee S, Banerji U. Exploiting the folate receptor alpha in oncology. *Nat Rev Clin Oncol.* 2020;17:349–359.
2. Parker N, Turk MJ, Westrick E, Lewis JD, Low PS, Leamon CP. Folate receptor expression in carcinomas and normal tissues determined by a quantitative radioligand binding assay. *Anal Biochem.* 2005;338:284–293.
3. Low PS, Kularatne SA. Folate-targeted therapeutic and imaging agents for cancer. *Curr Opin Chem Biol.* 2009;13:256–262.
4. Assaraf YG, Leamon CP, Reddy JA. The folate receptor as a rational therapeutic target for personalized cancer treatment. *Drug Resist Updat.* 2014;17:89–95.
5. Zhang Z, Wang J, Tacha DE, et al. Folate receptor alpha associated with triple-negative breast cancer and poor prognosis. *Arch Pathol Lab Med.* 2014;138:890–895.
6. Norton N, Youssef B, Hillman DW, et al. Folate receptor alpha expression associates with improved disease-free survival in triple negative breast cancer patients. *NPJ Breast Cancer.* 2020;6:4.
7. Pribble P, Edelman MJ. EC145: a novel targeted agent for adenocarcinoma of the lung. *Expert Opin Investig Drugs.* 2012;21:755–761.
8. Teng L, Xie J, Teng L, Lee RJ. Clinical translation of folate receptor-targeted therapeutics. *Expert Opin Drug Deliv.* 2012;9:901–908.
9. Xu L, Bai Q, Zhang X, Yang H. Folate-mediated chemotherapy and diagnostics: an updated review and outlook. *J Control Release.* 2017;252:73–82.
10. Farran B, Pavitra E, Kasa P, Peela S, Rama Raju GS, Nagaraju GP. Folate-targeted immunotherapies: passive and active strategies for cancer. *Cytokine Growth Factor Rev.* 2019;45:45–52.
11. Siegel BA, Dehdashti F, Mutch DG, et al. Evaluation of ^{111}In-DTPA-folate as a receptor-targeted diagnostic agent for ovarian cancer: initial clinical results. *J Nucl Med.* 2003;44:700–707.
12. Fisher RE, Siegel BA, Edell SL, et al. Exploratory study of ^{99m}Tc-EC20 imaging for identifying patients with folate receptor-positive solid tumors. *J Nucl Med.* 2008;49:899–906.
13. Low PS, Henne WA, Doorneweerd DD. Discovery and development of folic-acid-based receptor targeting for imaging and therapy of cancer and inflammatory diseases. *Acc Chem Res.* 2008;41:120–129.
14. Müller C. Folate based radiopharmaceuticals for imaging and therapy of cancer and inflammation. *Curr Pharm Des.* 2012;18:1058–1083.

15. Antony AC. Folate receptors. *Annu Rev Nutr.* 1996;16:501–521.
16. Yi YS. Folate receptor-targeted diagnostics and therapeutics for inflammatory diseases. *Immune Netw.* 2016;16:337–343.
17. Wang X, Shen F, Freisheim JH, Gentry LE, Ratnam M. Differential stereospecificities and affinities of folate receptor isoforms for folate compounds and antifolates. *Biochem Pharmacol.* 1992;44:1898–1901.
18. Maziarz KM, Monaco HL, Shen F, Ratnam M. Complete mapping of divergent amino acids responsible for differential ligand binding of folate receptors a and b. *J Biol Chem.* 1999;274:11086–11091.
19. Vaitilingam B, Chelvam V, Kularatne SA, Poh S, Ayala-Lopez W, Low PS. A folate receptor-alpha-specific ligand that targets cancer tissue and not sites of inflammation. *J Nucl Med.* 2012;53:1127–1134.
20. Müller C. Folate-based radiotracers for PET imaging: update and perspectives. *Molecules.* 2013;18:5005–5031.
21. Boss SD, Ametamey SM. Development of folate receptor-targeted PET radiopharmaceuticals for tumor imaging: a bench-to-bedside journey. *Cancers (Basel).* 2020;12:1508.
22. Almuhaideb A, Papathanasiou N, Bomanji J. ^{18}F-FDG PET/CT imaging in oncology. *Ann Saudi Med.* 2011;31:3–13.
23. Verweij NJF, Yaqub M, Bruijnen STG, et al. First in man study of [^{18}F]fluoro-PEG-folate PET: a novel macrophage imaging technique to visualize rheumatoid arthritis. *Sci Rep.* 2020;10:1047.
24. Betzel T, Müller C, Groehn V, et al. Radiosynthesis and preclinical evaluation of 3'-aza-2'-[^{18}F]fluorofolic acid: a novel PET radiotracer for folate receptor targeting. *Bioconjug Chem.* 2013;24:205–214.
25. Gnesin S, Müller J, Burger IA, et al. Radiation dosimetry of ^{18}F-AzaFol: a first in-human use of a folate receptor PET tracer. *EJNMMI Res.* 2020;10:32.
26. Boss SD, Müller C, Siwowska K, et al. Diastereomerically pure 6R- and 6S-3'-aza-2'-^{18}F-fluoro-5-methyltetrahydrofolates show unprecedentedly high uptake in folate receptor-positive KB tumors. *J Nucl Med.* 2019;60:135–141.
27. Deng Y, Wang Y, Cherian C, et al. Synthesis and discovery of high affinity folate receptor-specific glycinamide ribonucleotide formyltransferase inhibitors with antitumor activity. *J Med Chem.* 2008;51:5052–5063.
28. Müller C, Mindt TL, de Jong M, Schibli R. Evaluation of a novel radiofolate in tumour-bearing mice: promising prospects for folate-based radionuclide therapy. *Eur J Nucl Med Mol Imaging.* 2009;36:938–946.
29. Müller C, Forrer F, Schibli R, Krenning EP, de Jong M. SPECT study of folate receptor-positive malignant and normal tissues in mice using a novel ^{99m}Tc-radiofolate. *J Nucl Med.* 2008;49:310–317.
30. Gu Z, Taschereau R, Vu NT, et al. Performance evaluation of G8, a high-sensitivity benchtop preclinical PET/CT tomograph. *J Nucl Med.* 2019;60:142–149.
31. Siwowska K, Schmid RM, Cohrs S, Schibli R, Müller C. Folate receptor-positive gynecological cancer cells: in vitro and in vivo characterization. *Pharmaceuticals (Basel).* 2017;10:72.
32. Lorusso PM, Edelman MJ, Bever SL, et al. Phase I study of folate conjugate EC145 (vintafolide) in patients with refractory solid tumors. *J Clin Oncol.* 2012;30:4011–4016.
33. Luyckx M, Votino R, Squifflet JL, Baurain JF. Profile of vintafolide (EC145) and its use in the treatment of platinum-resistant ovarian cancer. *Int J Womens Health.* 2014;6:351–358.
34. Sato S, Itamochi H. Profile of farletuzumab and its potential in the treatment of solid tumors. *Onco Targets Ther.* 2016;9:1181–1188.
35. Moore KN, Martin LP, O'Malley DM, et al. A review of mirvetuximab soravtansine in the treatment of platinum-resistant ovarian cancer. *Future Oncol.* 2018;14:123–136.
36. Morris RT, Joyrich RN, Naumann RW, et al. Phase II study of treatment of advanced ovarian cancer with folate-receptor-targeted therapeutic (vintafolide) and companion SPECT-based imaging agent (^{99m}Tc-etarfolatide). *Ann Oncol.* 2014;25:852–858.
37. Kamen BA, Smith AK. A review of folate receptor alpha cycling and 5-methyltetrahydrofolate accumulation with an emphasis on cell models in vitro. *Adv Drug Deliv Rev.* 2004;56:1085–1097.